Evaluation of the Vickers microhardness and fracture toughness on hot pressed Bi-2212/Ag ceramic composites

F. Kahraman

Journal of Materials Science: Materials in Electronics

ISSN 0957-4522

J Mater Sci: Mater Electron
DOI 10.1007/s10854-016-4796-7

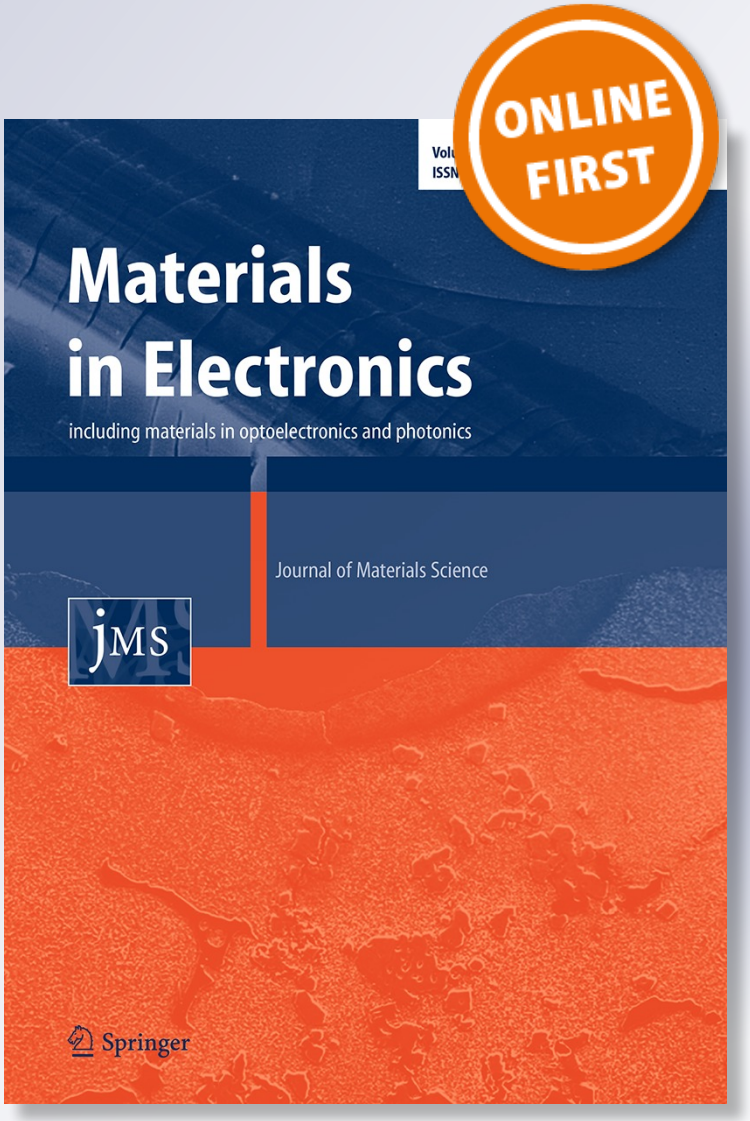

Springer

J Mater Sci: Mater Electron
DOI 10.1007/s10854-016-4796-7

Evaluation of the Vickers microhardness and fracture toughness on hot pressed Bi-2212/Ag ceramic composites

F. Kahraman[1]

Received: 16 February 2016 / Accepted: 7 April 2016

Abstract Micro-indentation tests provide useful information on mechanical properties such as strength, deformation characteristics and fracture toughness of the ceramic materials. Therefore, a micro-indentation study has been carried out to characterize the mechanical properties of $Bi_2Sr_2Ca_1Cu_2O_{8+\delta}$ + x wt % Ag (x = 0.0, 0.05, 0.15, 0.25 and 0.50) samples fabricated by hot pressing technique. Vickers hardness, elastic modulus, elastic stiffness coefficient, brittleness index, yield strength, compressive strength, and fracture toughness values of the samples were determined by using apparent micro-hardness. Additionally, load independent values of elastic modulus, elastic stiffness coefficient, brittleness index, yield strength and fracture toughness were also improved by using true microhardness. The experimental results have been analyzed by the theoretical models being proposed in the literature (Meyer's Law, the elastic/plastic deformation model, proportional sample resistance model, Hays–Kendall model). According to the obtained results, Hays–Kendall model was determined to be as the most suitable model in the plateau region for the all samples showing indentations size effect behavior. The results show that the values of microhardness, strength, elastic parameters and fracture toughness of the samples increased with an increase in the Ag addition. The results exhibit that, it is possible to control the mechanical properties of the Bi-2212 ceramic composites by increasing the Ag addition

✉ F. Kahraman
fundakahraman33@hotmail.com

[1] Department of Mechatronics Engineering, Faculty of Tarsus Technology, Mersin University, Mersin, Turkey

1 Introduction

The mechanical properties such as hardness, strength, elasticity, fracture toughness as well as magnetic, electric and superconducting properties of high temperature oxide superconductors are very important for many technological applications [1]. Due to their brittle nature and the weak links between grains, the poor mechanical characteristics of this kind of materials imposes limitations for fabrication wires and tapes [2]. Some attempts to improve their mechanical properties have been performed by means of Ag addition on Bi–Sr–Ca–Cu–O (BSCCO) compounds [3–8]. There have been many publications written on the electrical, magnetic and structural properties of BSCCO however not enough can be found about mechanical properties [9–16]. The mechanical properties of materials depend on their internal structure. To improve mechanical properties, internal structure modifications can be improved extremely with different substitution/addition of dopants or by means of heat treatment such as atmospheric annealing or vacuum treatment [17, 18]. Microhardness is not only measured for determining mechanical characteristic of materials but it has also been developed as an investigation method of structural parameters. Regarding mechanical properties, hardness tests provide useful information on the strength and deformation properties of the materials. A simple, quick, efficient, sensitive and non-destructive method to evaluate the mechanical properties of ceramic materials is the Vickers indentation hardness measurement has been used widely in industry. In the previous studies were proposed to investigate the relationship between the applied load or content and the microhardness results of ceramic materials [19]. The most of researcher suggested that different materials indicate differently microhardness characterization depending on

Published online: 11 April 2016

applied load. It is reported that microhardness is independent of load, increases or decreases with load, shows different variation with changes in the load [20].

This experimental study was carried out to determine load dependent and independent Vickers micro-hardness, Elastic modulus, yield strength, and fracture toughness for Bi-2212 with different amounts of Ag addition. Micro-indentation technique has been performed on Bi-2212/Ag ceramics fabricated by hot pressed method. The effect of Ag addition on mechanical properties has been investigated. Furthermore, the load dependency of microhardness has been examined according to the several empirical models: Meyer's law, proportional sample resistance model (PSR), elastic–plastic deformation model (EPD), Hays–Kendall model (HK) proposed in literature. The fundamental concern of this study was to determine the load dependent and load independent mechanical properties and to investigate the effect of Ag addition on the mechanical properties of Bi-2212 samples.

2 Materials and methods

Initial samples have been prepared by cold pressing at about 250 MPa for 2 min from $Bi_2Sr_2Ca_1Cu_2O_{8+\delta}$ powders prepared by the standard solid-state reaction method using high purity chemicals Bi_2O_3 (99.99 %), $SrCO_3$ (99.9+ %), $CaCO_3$ (99+ %), CuO (99+ %) powders, and x wt % Ag (x = 0.0, 0.05, 0.15, 0.25 and 0.50). These samples were subsequently hot-pressed at around 20 MPa at 800 °C for 12 h by using cylindrical die. The produced hot- pressed discs are 25 mm diameter and 2 mm thick. After the hot-pressing process, the discs were annealed for 72 h at 860 °C to recover the Bi-2212 phase, followed by 24 h at 800 °C to adjust the oxygen content and, finally, quenched in air to room temperature. This process is necessary as at 800 °C under pressure, Bi-2212 phase is partially decomposed in Bi-2201 and secondary phases [3]. Samples with 0, 0.05, 0.15, 0.25 and 0.50 wt % Ag after this will be named as A_0, A_1, A_2, A_3 and A_4, respectively. The microhardness measurements were performed for characterization of mechanical properties of Bi-2212/Ag ceramics. Vickers microhardness of the studied samples were measured using ZHVμ series Zwick microhardness measurement device at room temperature. Vickers indenter that is made from diamond with a shape of square pyramid applied on the cleaned and polished surfaces of the samples under loads varying from 0.245 to 4.9 N for 15 s. The pyramidal indenter is also applied the different locations on the samples to avoid surface effects and overlap. For statistical reasons, 5 indentations were made under each load and the arithmetic mean of the measured values was taken as result. The diagonal lengths of indentation were measured with an accuracy to be ±0.1 μm.

3 Results and discussion

3.1 Vickers microhardness measurements

Hardness that is defined as the resistance against to plastic deformation, indentation or penetration by means such as abrasion, cutting, scratching, drilling and wear of the materials [21]. It has a relationship between other mechanical properties such as elastic modulus, yield strength. Elastic modulus and yield strength can be theoretically computed by the using hardness values. Elastic modulus is a measure of elastic deformation under the force. It can be defined by the ratio of strength to strain. The elastic modulus is defined as the slope of its strain–stress curve in the elastic deformation region. Yield strength is the ratio of magnitude of the external force to the cross-sectional area in the elastic region. Compressive strength is the ratio of magnitude of the external force to the cross-sectional in the plastic region. Elastic stiffness is resistance to deformation or strain. Elastic stiffness coefficient gives the idea of tightness of bonding between neighboring atoms. Brittleness index that represents ductility of material is defined as the property of rupture without plastic deformation. Strength intensity factor, K_{IC} is referred to as fracture toughness, is one of the most important properties of any material for many design applications. It is a property which describes the resistance of a material containing a crack to resist propagation and fracture.

Vickers microhardness (apparent) is calculated using the Eq. 1.

$$H_V = 1854.4F/d^2 \tag{1}$$

where H_v is microhardness in (Pa), F is applied load in (N) and d is the mean diagonal length of the indentation impression in (μm).

In most materials, the elastic modulus, E is related to the Vickers microhardness (apparent) by the relation,

$$E = 81.9635H_V \tag{2}$$

Elastic stiffness coefficient (C_{11}) and brittleness index (B_i) can be theoretically computed by the using hardness values,

$$C_{11} = H_V^{7/4} \tag{3}$$

$$B_i = H_v/K_{IC} \tag{4}$$

Yield strength (σ_y) and compressive strength (σ_c) are calculated using the following expressions,

$$\sigma_y \approx H_V/3 \quad (5)$$

$$\sigma_C = F/A \quad (6)$$

where F is applied force and A is cross-sectional area of indentation mark.

According to the definition of K_{IC} as the critical strength intensity factor, it is directly related to the surface energy, γ, of the crack faces.

$$K_{IC} = \sqrt{2E\gamma} \quad (7)$$

The values of H_v, E, σ_y, σ_c, C_{11}, K_{IC}, and B_i values were calculated as a function of the load and listed in Table 1. From this table, it was observed that increases H_v, E, σ_y, σ_c, C_{11} and K_{IC} values of the all samples with increasing Ag additions. Wheras B_i decreases with increasing Ag additions.

Figure 1 shows the variation H_v the as a function of Ag addition for the samples. It is observed that from Fig. 1, the microhardness values increased with increasing Ag addition.

The variation of H_v as a function of the applied loads, F (N) for the samples is given in Fig. 2. It can be seen from the curves in Fig. 2 that H_v values are load dependent. This indicates that the hardness value depends on the applied load and there is a relation between the load and size of the indenter. The dependence of the load showed that indentation size effect (ISE) has an effect on the samples. H_v values decrease non-linearly as the applied load increased, and then these reach a plateau region at around 1.96 N for all studied samples. After this value changes in the microhardness value will be insignificant. This non-linear behavior has also been observed in the literature for

Table 1 Load dependent H_v, E, σ_y, σ_c, C_{11}, K_{IC} and B_i values for the samples

Samples	F (N)	d (μm)	H_v (GPa)	E (GPa)	σ_y (GPa)	σ_c (GPa)	C_{11} (GPa)	K_{IC} (GPam$^{1/2}$)	B_i (m$^{-1/2}$)
A_0	0.245	31.081	0.478	39.179	0.159	0.514	0.274	0.482	0.991
	0.490	49.895	0.365	29.917	0.122	0.394	0.171	0.421	0.866
	0.980	75.125	0.322	26.392	0.107	0.347	0.137	0.395	0.815
	1.960	108.11	0.311	25.491	0.104	0.335	0.129	0.388	0.801
	2.940	134.81	0.300	24.589	0.100	0.323	0.121	0.381	0.787
	4.900	175.50	0.295	24.179	0.098	0.318	0.118	0.378	0.780
A_1	0.245	30.174	0.499	40.899	0.166	0.538	0.296	0.520	0.959
	0.490	48.645	0.384	31.474	0.128	0.414	0.187	0.458	0.838
	0.980	72.578	0.345	28.277	0.115	0.372	0.155	0.432	0.798
	1.960	104.95	0.330	27.048	0.110	0.365	0.143	0.423	0.780
	2.940	130.12	0.322	26.392	0.107	0.347	0.137	0.418	0.770
	4.900	169.84	0.315	25.818	0.105	0.340	0.132	0.413	0.762
A_2	0.245	28.922	0.543	45.244	0.184	0.595	0.343	0.589	0.937
	0.490	46.792	0.415	34.015	0.138	0.447	0.214	0.510	0.813
	0.980	71.248	0.358	29.343	0.119	0.385	0.165	0.474	0.755
	1.960	102.94	0.343	28.113	0.114	0.360	0.153	0.464	0.739
	2.940	128.15	0.332	27.212	0.111	0.358	0.145	0.456	0.728
	4.900	167.46	0.324	26.556	0.108	0.349	0.139	0.451	0.718
A_3	0.245	28.387	0.563	46.965	0.191	0.618	0.372	0.643	0.884
	0.490	44.541	0.458	37.539	0.158	0.494	0.254	0.575	0.796
	0.980	69.522	0.375	30.818	0.125	0.405	0.179	0.521	0.737
	1.960	101.62	0.351	28.851	0.173	0.380	0.160	0.504	0.698
	2.940	127.00	0.338	27.704	0.113	0.364	0.149	0.494	0.684
	4.900	165.18	0.333	27.293	0.111	0.359	0.145	0.490	0.679
A_4	0.245	27.987	0.580	47.538	0.193	0.625	0.385	0.675	0.859
	0.490	44.015	0.469	38.358	0.156	0.506	0.265	0.607	0.772
	0.980	67.570	0.398	32.621	0.133	0.429	0.199	0.559	0.711
	1.960	100.62	0.369	30.244	0.123	0.387	0.174	0.538	0.685
	2.940	124.62	0.351	28.769	0.117	0.379	0.160	0.525	0.668
	4.900	161.35	0.349	28.605	0.116	0.376	0.158	0.524	0.666

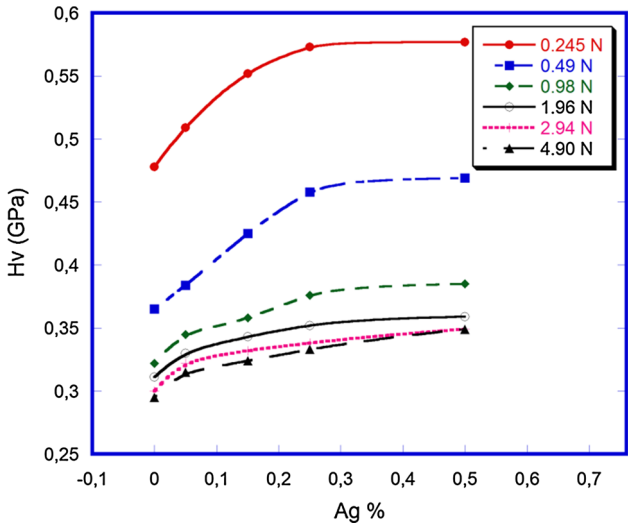

Fig. 1 The variation of apparent microhardness with Ag % content

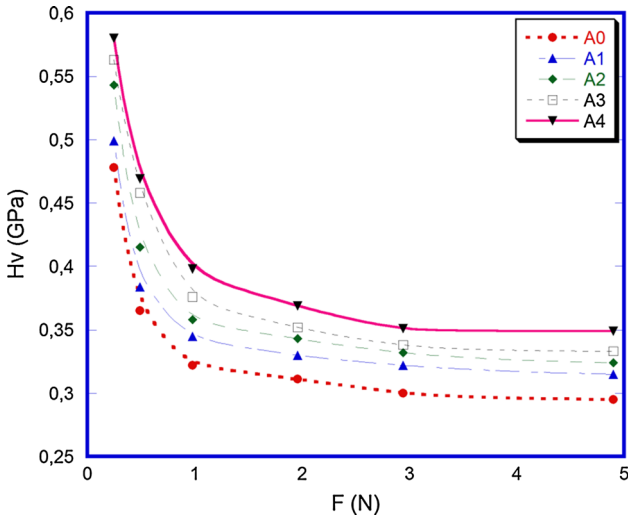

Fig. 2 The variation of apparent microhardness with applied load

BSCCO samples and is known as ISE [22, 23]. The penetration depth increases at higher loads (F > 1.96 N) and the effect of inner layers becomes more important. There are several models to describe the ISE behavior such as Meyer's law, Hays–Kendall (HK) model, elastic/plastic deformation (EPD) model and proportional specimen resistance model (PSR) [18, 22, 23].

3.2 Analysis and modeling

3.2.1 Analysis according to Meyer's law

Meyer's law is frequently used model to explain the ISE and reverse indentation size effect (RISE) behavior of materials. There is a relationship between applied load and diagonal length of indentation in this law.

$$F = Ad^n \tag{8}$$

where F is applied load, d is indentation diagonal length, n is Meyer's number A is the standard hardness constant.

The value of n is used a measure of ISE or RISE. ISE behavior occurs when the n value is <2, indicating that the hardness increases with decreasing of the applied load, if n value is greater than 2, RISE behavior is obtained, indicating that the hardness increase with increasing the applied load. When n is equal 2, hardness is independent from the applied load [18].

The values of n and A can be obtained from the plots of $ln\ F$ versus $ln\ d$ for all the samples. The slope of the $ln\ F$-$ln\ d$ graph gives n and vertical intercept is proportional to A. The results obtained from the samples and linear regression coefficient, r^2 are given in Table 2. Each set of data shows an excellent linear relationship. From Table 2, it can be noticed that Meyer number is less than 2 for the all samples, which proves load dependent displacement has ISE behavior.

3.2.2 Analysis according to Hays–Kendall model

In this model, Hays–Kendall's law which proposes that when the load, F is applied to the specimen, the load is partially affected by a small sample resistance pressure F_0, which is a function of the material under investigation. According to modified Hays and Kendall's law, the effective indentation load, $F_{eff} = F–F_0$ is related with the load independent hardness (true hardness, H_0) by the following formula:

$$H_0 = 1854.4\left(\frac{F - F_0}{d^2}\right) \tag{9}$$

The values of sample resistance pressure, F_0 and true hardness (load independent hardness), H_0 can be obtained from the plots of F versus d^2 for all the samples. The slope of each line allows to obtain H_0, and the intercept of each

Table 2 Regression analysis of experimental data according to Meyer's law

Samples	n	ln A (GPa)	r^2	H_v (GPa)
A_0	1.74	−7.474	0.99859	0.295–0.300
A_1	1.75	−7.457	0.99847	0.315–0.322
A_2	1.72	−7.264	0.99843	0.324–0.332
A_3	1.69	−7.107	0.99872	0.333–0.338
A_4	1.70	−7.138	0.99893	0.349–0.351

line represents, F_0. The values of H_0, F_0 and r^2 were summarized in Table 3.

3.2.3 Analysis according to proportional specimen resistance (PSR) model

It is observed that the diagonal length is strongly depends on the applied load from the empirical observations, which is given by

$$\frac{F}{d} = \gamma + H_0\, d \tag{10}$$

The values of H_0 and can be obtained from the plots of F versus d^2 for all the samples. The slope of each line corresponds to the true hardness, H_0, and the intercept of each line represents the surface energy, γ. The extracted values of H_0, and r^2 were listed in Table 4. As can be seen from the table, H_0 values of the samples increased with increasing Ag content.

3.2.4 Analysis according to elastic/plastic deformation (EPD) model

Applied load dependence of indentation length can be determined by using Eq. 11.

$$H_0 = 1854.4\left(\frac{F}{(d_p + d_e)^2}\right) \tag{11}$$

where de elastic deformation is in accordance with the d_p plastic deformation. d_e is computed by plotting $F^{1/2}$ against the indentation length d.

The load dependence of indentation diagonal lengths for samples was analyzed as $F^{1/2}$ against d_p plots. The values of H_0 and d_e can be obtained from the plots of square root of applied load, $F^{1/2}$ versus the impression diagonal length, d_p for all the samples. The slope of each curve is proportional to H_0, and the intercept of this curve is proportional to the elastic part of the indentation semi diagonal, d_e. The extracted values of H_0 and de and r^2 are listed in Table 5. As can be seen from this table. The value of d_e is positive for all samples. That means for this range of applied loads elastic deformation is obtained along with plastic deformation. Presence of elastic deformation along with plastic deformation is the reason of ISE behavior for these samples.

The values of load independent H_0, E, σ_y, C_{11}, K_{IC} and B_i were calculated using true hardness for each samples for HK PSR and EPD models and results listed in Tables 6, 7 and 8, respectively. From these tables, it was observed that the load independent values of H_0, E, σ_y, C_{11} and K_{IC} increase with increasing the Ag concentration, while B_i decreases with increasing the Ag concentration.

Furthermore, load independent hardness, H_0, calculated according to Eqs. (9–11) and percentage error for HK, PSR and EPD models was calculated and listed in Table 9. Table 9 shows the variation of the experimental results, and theoretical true microhardness for different models. Percentage error was determined as (1.57–3.42) for HK model, (9.74–13.14) for EPD model, (52.52–56.85) for PSR model. Minimum percentage error was obtained for HK model in the given range of the applied load. The hardness value obtained with HK model is similar the hardness value in the plateau region. So, the HK model is the most suitable model in the analysis microhardness and determining the mechanical properties of all the studied samples. The comparisons of load dependent and load independent H_0, E, σ_y, C_{11}, K_{IC} and B_i values for HK model is given in Table 10. From this table, the load dependent values of H_v, E, σ_y, C_{11}, K_{IC} and B_i are greater than that of load independent values. H_0, E_0, σ_{y0}, C_{110}, K_{IC0} and B_{i0} values increased with increasing Ag addition, whereas B_{i0}

Table 3 Regression analysis of experimental data according to HK model

Samples	F_0 (N)	H_0 (GPa)	r^2	H_v (GPa)
A_0	0.105	0.290	0.99996	0.295–0.300
A_1	0.093	0.313	0.99999	0.315–0.322
A_2	0.118	0.317	0.99995	0.324–0.332
A_3	0.132	0.324	0.99996	0.333–0.338
A_4	0.120	0.338	0.99993	0.349–0.351

Table 4 Regression analysis of the experimental data according to PSR model

Samples	H_0 (GPa)	$\gamma \times 10^{-3}$ (N/μm)	r^2	H_v (GPa)
A_0	0.141	2.965	0.99886	0.295–0.300
A_1	0.146	3.315	0.99767	0.315–0.322
A_2	0.147	3.836	0.99748	0.324–0.332
A_3	0.148	4.413	0.99890	0.333–0.338
A_4	0.151	4.801	0.99892	0.349–0.351

Table 5 Regression analysis of the experimental data according to EPD model

Samples	H_0 (GPa)	d_e (μm)	r^2	H_v (GPa)
A_0	0.265	8.995	0.99986	0.295–0.300
A_1	0.287	8.041	0.99981	0.315–0.322
A_2	0.288	9.545	0.99986	0.324–0.332
A_3	0.291	10.604	0.99987	0.333–0.338
A_4	0.304	10.011	0.99977	0.349–0.351

Table 6 The calculated load independent H_0, E, σ_y, C_{11}, K_{IC} and B_i values for HK model

Samples	H_0 (GPa)	E (GPa)	σ_y (GPa)	C_{11} (GPa)	K_{IC} (GPam$^{1/2}$)	B_i (m$^{-1/2}$)
A_0	0.290	23.769	0.096	0.114	0.375	0.773
A_1	0.313	25.654	0.104	0.130	0.412	0.759
A_2	0.317	25.982	0.105	0.133	0.446	0.710
A_3	0.324	26.556	0.108	0.139	0.484	0.669
A_4	0.338	27.703	0.112	0.149	0.515	0.656

Table 7 The calculated load independent H_0, E, σ_y, C_{11}, K_{IC} and B_i values for PSR model

Samples	H_0 (GPa)	E (GPa)	σ_y (GPa)	C_{11} (GPa)	K_{IC} (GPam$^{1/2}$)	B_i (m$^{-1/2}$)
A_0	0.141	11.556	0.047	0.0324	0.261	0.540
A_1	0.146	11.966	0.048	0.0344	0.281	0.519
A_2	0.147	12.049	0.049	0.0348	0.304	0.483
A_3	0.148	12.130	0.049	0.0353	0.327	0.452
A_4	0.151	12.376	0.050	0.0365	0.344	0.438

Table 8 The calculated load independent H_0, E, σ_y, C_{11}, K_{IC} and B_i values for EPD model

Samples	H_0 (GPa)	E (GPa)	σ_y (GPa)	C_{11} (GPa)	K_{IC} (GPam$^{1/2}$)	B_i (m$^{-1/2}$)
A_0	0.265	21.720	0.088	0.0978	0.358	0.740
A_1	0.287	23.523	0.095	0.112	0.394	0.728
A2	0.288	23.605	0.096	0.113	0.425	0.677
A3	0.291	23.851	0.097	0.115	0.458	0.635
A4	0.304	24.916	0.101	0.124	0.489	0.621

Table 9 Average Vickers microhardness (H_v) in plateau region, and theoretical true microhardness (H_0) and error (%) values for HK, PSR and EPD models

Samples	H_{0HK} (GPa)	Error (%)	H_{0PSR} (GPa)	Error (%)	H_{0EPD} (GPa)	Error (%)	H_v (GPa)
A_0	0.290	2.35	0.141	52.52	0.265	10.77	0.297
A_1	0.313	1.57	0.146	54.08	0.287	9.74	0.318
A_2	0.317	3.35	0.147	55.18	0.288	12.19	0.328
A_3	0.324	3.28	0.148	55.82	0.291	13.13	0.335
A_4	0.338	3.42	0.151	56.85	0.304	13.14	0.350

Table 10 Load dependent, and load independent H_0, E, σ_y, C_{11}, K_{IC} *and* B_i values for HK model

Samples	A_0	A_1	A_2	A_3	A_4
H_v (GPa)	0.297	0.318	0.328	0.335	0.350
H_0 (GPa)	0.290	0.313	0.317	0.324	0.338
E (GPa)	24.343	26.064	26.884	27.457	28.687
E_0 (GPa)	23.769	25.654	25.982	26.556	27.703
σ_y (GPa)	0.099	0.106	0.109	0.111	0.116
σ_{y0} (GPa)	0.096	0.104	0.105	0.108	0.112
C_{11} (GPa)	0.119	0.134	0.142	0.147	0.159
C_{110} (GPa)	0.114	0.130	0.133	0.139	0.149
K_{IC} (GPam$^{1/2}$)	0.379	0.415	0.454	0.492	0.524
K_{IC0} (GPam$^{1/2}$)	0.375	0.412	0.446	0.484	0.515
B_i (m$^{-1/2}$)	0.783	0.766	0.722	0.680	0.667
B_{i0} (m$^{-1/2}$)	0.773	0.759	0.710	0.669	0.656

decreases with increasing Ag addition indicating that the samples become more toughness and more hard and ductile.

4 Conclusions

In this study, the effect of Ag addition on the mechanical properties such as microhardness, elastic modulus, elastic stiffness coefficient, brittleness index, yield strength and fracture toughness of Bi-2212 ceramic composites has been investigated. Results show that Ag addition has a positive effect on the mechanical properties of Bi-2212 samples. The experimental results of the microhardness measurements have been also analyzed using Meyer's law, HK, PSR and EPD models. Load independent microhardness, elastic modulus, elastic stiffness coefficient, yield strength fracture toughness, of the samples were evaluated. HK

model was determined as the most successful model for the samples. The predicted values were found to be statistically similar to the actual measured values in the plateau region. The Vickers microhardness, elastic parameters and fracture toughness of samples were improved with increasing Ag addition. These enhancement are believed to be due to the presence of Ag particles that can encourage compressive stresses in the superconducting matrix and resist crack propagation by pinning the propagating cracks, and it is associated to the formation of liquid phase during the hot pressing process and the reinforcement of the weak links by Ag, as reported in previous works [24–26].

References

1. U. Kölemen, O. Uzun, M. Yılmazlar, N. Güçlü, E. Yanmaz, J. Alloy. Compd. **415**, 300 (2006)
2. S. Cavdar, E. Deniz, H. Koralay, O. Ozturk, M. Erdem, A. Gunen, J. Supercond. Nov. Magn. **25**, 2297 (2012)
3. F. Kahraman, A. Sotelo, M.A. Madre, J.C. Diez, B. Ozkurt, Sh Rasekh, Ceram. Int. **41**, 14924 (2015)
4. A. Salazar, J.Y. Pastor, J. Llorca, Physica C **358**, 404 (2003)
5. A. Sotelo, M. Mora, M.A. Madre, J.C. Diez, L.A. Angurel, G.F. de la Fuente, J. Eur. Ceram. Soc. **25**, 2947 (2005)
6. M. Mora, A. Sotelo, H. Amaveda, M.A. Madre, J.C. Diez, L.A. Angurel, G.F. de la Fuente, Bol. Soc. Esp. Ceram. **44**, 199 (2005)
7. M.A. Madre, H. Amedava, M. Mora, A. Sotelo, L.A. Angurel, J.C. Diez, Bol. Soc. Esp. Ceram. **47**(3), 148 (2008)
8. Q.B. Hao, C.S. Li, S.N. Zhang, J.Q. Feng, M.H. Du, Physica C **471**, 1100 (2011)
9. A.Y. Ilyushechkina, I.E. Agranovski, I.S. Altman, M. Choic, Mater. Sci. Eng., B **167**, 60 (2010)
10. R.H. Patel, A. Nabialek, M. Niewczas, Supercond. Sci. Technol. **18**, 317 (2005)
11. E.A. Duarte, P.A. Quintero, M.W. Meisel, J.C. Nino, Physica C **495**(15), 109 (2013)
12. V. Garnier, R. Caillard, A. Sotelo, G. Desgardin, Physica C **319**, 197 (1999)
13. F.M. Costa, Sh Rasekh, N.M. Ferreira, A. Sotelo, J.C. Diez, M.A. Madre, J. Supercond. Nov. Magn. **26**, 943 (2013)
14. M.M. Ibrahim, N.M. Megahid, M.M.A. El-Raheem, S.M. Khalil, New J. Glass Ceram. **2**(2), 75 (2012)
15. X.Y. Lu, D. Yi, H. Chen, A. Nagata, Phys. Procedia **27**, 260 (2012)
16. M.Z. Shoushtari, A. Bahrami, M. Farbod, Phys. Status Solidi C **3**(9), 2994 (2006)
17. M. Tosun, S. Ataoglu, L. Arda, O. Ozturk, E. Asikuzun, D. Akcan, O. Cakiroglu, Mater. Sci. Eng., A **590**, 416 (2014)
18. S.M. Khalil, A.M. Ahmed, Physica C **452**, 21 (2007)
19. J.K.M.F. Daguna, P.A. Suzuki, K. Strecker, M.H.F.V. Fernandes, C. Santos, Mater. Sci. Eng. A **533**, 26 (2012)
20. S.M. Khalil, AIP Adv **2**, 042183 (2012)
21. W.F. Smith, *Principles of Materials Science and Engineering*, 2nd edn. (Mc Graw-Hill Companies Inc., NY, 1990)
22. N. Nursoy, M. Yilmazlar, C. Terzioglu, I. Belenli, J. Alloy. Compd. **459**, 399 (2008)
23. M. Yılmazlar, O. Ozturk, O. Görür, I. Belenli, C. Terzioğlu, Superconduct. Sci. Technol. **20**, 365 (2007)
24. W. Abdeen, N.H. Mohammed, R. Awad, S.A. Mahmoud, M. Hasebbo, J. Supercond. Nov. Magn. **26**, 3235 (2013). doi:10.1007/s10948-013-2192-6
25. J. Joo, J.P. Singh, T. Warzynski, A. Grow, R.B. Poeppel, Appl. Supercond. **2**(6), 401 (1994)
26. A. Sotelo, M.A. Madre, J.C. Diez, Sh Rasekh, L.A. Angurel, E. Martinez, J. Supercond. Sci. Technol. **22**, 034012 (2009)